MECSOL 2022 - Proceedings of the 8th International Symposium on Solid Mechanics
M.L. Bittencourt, J. Labaki, L.C.M. Vieira Jr. and E. Mesquita (Editors), Campinas SP, Brazil, October 17th to 19th, 2022

Evaluation of Friction at the Chip-Tool Interface in Orthogonal Cutting by Mechanistic Models applied to Limit Analysis

Luísa de Amorim Makhoul Gomes[2], Fabio da Costa Figueiredo[2], Lívia Mendonça Nogueira [1,2] and Adriane Lopes Mougo[1]

[1] Federal Center for Technological Education Celso Suckow da Fonseca, Campus Nova Iguaçu, Rio de Janeiro, Brazil
[2] Federal University of Rio de Janeiro, Rio de Janeiro, Brazil.

Abstract: In oil industry, equipment are submitted to high pressures and temperatures. Often, corrosive fluids flow over them, requiring the use of materials with high mechanical resistance allied to corrosion resistance. Then, Superduplex steels are commonly used in these applications. Regarding manufacturing of such components, these steels present low machining and special tools are required. Experimental evaluation of cutting forces are costly and time consuming and in this case, it is more severe. Also, friction at chip-tool interface plays an important role in cutting forces evaluation. Due to these factors, this work proposes a mechanistic model considering the data from AISI 316 and 410 steels in order to determine the Superduplex friction coefficient due to their low cost and they can simulate the Superduplex microstructure. This Superduplex friction coefficient is calibratated from a mechanistic model using data from the other steels. This calibrated friction coefficient is then applied in a limit analysis model and the numerical and experimental results are compared. In this simulation, the required permanent regime configuration is determined from Merchant's model. The simulation is carried out by discretizing the specimen into finite elements and at permanent regime configuration, the tool-specimen contact region is supposed known and modeled by Kachanov theory. Numerical velocity and stress fields are obtained as well as cutting forces and tool-chip contact stresses.
Keywords: orthogonal cutting, friction, mechanistic model, limit analysis.

INTRODUCTION

Superduplex Steel (SS) are mostly used in oil industry due to its high strength allied to corrosion resistance. On the other hand, this material presents low machining and manufacturing requires special tools. The experimental determination of cutting forces is expensive and time consuming since it depends on numerous variables such as material properties, cutting parameters, chip-tool frictional contact conditions, contact length, tool material and the machine tool rigidity that acts directly on the cutting dynamics. Regarding SS, it is even more expensive and time consuming due to material features. Moreover, friction at tool-chip interface plays an important rule in the evaluation of cutting forces. The prediction of friction coefficient is difficult due to the lack of control of the chip-tool contact length and uncertainties about the effective chip area in contact with the rake tool surface. This effective area depends on the microscopic irregularities of the surfaces.

Among these factors, the chip-tool contact length is the most hard to determine. Its determination would help the understanding of friction on the rake surface during the chip flow, determination of other parameters such as average stresses during the flow process, prediction of tool life, evaluation of tool wear and temperatures due to heat generation during the metal cutting process influenced by the chip formation mechanism. According to Grzesik (2008), the contact length is one of the most important parameters in controlling the cutting process. If the contact length is reduced, it results in a substantial reduction in energy consumption, machined surface integrity, higher tool life, lower interface temperature and efficient chip control. In the literature, there are many models to calculate the chip-tool contact length (l_c) (Grzesik, 2008; Fatima and Mativenga, 2013):

- Modelo de Lee e Schaffer

$$\frac{l_c}{h} = \frac{\sqrt{2}}{sen\left[tg^{-1}\left(\frac{cos\gamma_0}{k_h - sen\gamma_0}\right) sen\left[45^o + tg^{-1}\left(\frac{cos\gamma_0}{k_h - sen\gamma_0}\right) - \gamma_0\right]\right]} \tag{1}$$

- Modelo de Abuladze

$$\frac{l_{st}}{h} = \left(\frac{h_{ch}}{h}\right)^{0,1} \left[\frac{h_{ch}}{h}(1 - tg\gamma_o) + \frac{1}{cos\gamma_o}\right] \tag{2}$$

- Modelo de Boothroyd e Bailey

$$\frac{l_c}{h} = \frac{cos(\phi - \gamma_0)[cos(\Theta - \gamma_0) + 2sen(\Theta - \gamma_0))]}{sen\phi[2(cos\Theta cos\gamma_o) + sen(\Theta - \gamma_0)]} \tag{3}$$

where ϕ is the shear plane angle, Θ is the friction angle, h is the cut thickness, h_{ch} is the cut nominal thickness, k_h is the cut nominal thickness and γ_0 is the rake angle.

The use of numerical models to simulate cutting operations may help the understanding of the phenomena and the observation of local responses, not captured by experimental devices. Once calibration such models, other cutting conditions may be evaluated by computational simulation. One of these techniques, limit analysis takes place. According to Figueiredo and Borges (2020), limit analysis theory is a direct method and is convenient if the interest is determination of the ultimate load-carrying of a body or structure: the plastic collapse at a permanent regime configuration. This state is achieved by looking directly at plastic collapse state without any need to follow loading steps as in incremental methods. In this work, a limit analysis methodology considering frictional contact between a rigid (tool) and a deformable body (workpiece) is considered. The permanent regime configuration is determined by Merchant model. As results, the cutting forces, contact stresses, velocity and stress fields are evaluated as well as the occurrence of sticking/sliding at tool-chip interface. The workpiece is a von Mises material under plane strain hypothesis and Coulomb friction law is used at chip-tool interface.

Based on these premises, the aim of this paper is to compare the experimental and numerical cutting forces in orthogonal cutting process. The friction coefficient to be applied in the model is determined in two stages: (i) from a mechanistic model considering AISI 316, AISI 410 and UNS S 32760 steels; (ii) from a linear model which the results for AISI 316 and AISI 410 steels will be used to predict the friction coefficient for superduplex steel (UNS S 32760). Besides friction coefficient, others parameters are necessary to build the numerical model: the contact length and the cutting width, the shear plane angle determined by Merchant's model and for the chip thickness will be measured with the assistance of the SEM.

EXPERIMENTAL PROCEDURE

The workpieces were composed by AISI 316, AISI 410 and superduplex UNS S32760 steels. The material properties are presented in Table 1. The turning process was carried out with a conventional Nardini lathe, model MS 205X1000. A Kistler dynamometer, model 9257BA, was used for acquisition machining forces, as observed in Fig. 1. This dynamometer measures forces in x, y and z axes with a sensitivity of 10 mV/N for x, y axes and 5.0 mV/N to z axis. With this sensor it is possible to measure the feed force F_f (x direction), the passive force F_p (y direction) and the cut F_c (z direction). The signals from the dynamometer are transferred to a Kistler Model 5233A1 3 channel signal conditioner, $\pm$5V output signal and built-in filter with cutting frequency of 200 Hz.

Table 1 – Mechanical properties

Steel	Hardness (HB)	Tensile strength (MPa)	σ_Y (MPa)
AISI 316	177	623	285
AISI 410	188	448	293
UNS S32760	247	680	591

To execute the cutting process, a cutting tool (insert) recommended for turning of stainless steel was used. The tool holder used was the S16R STFCR-11. The insert chosen was carbide from Mitsubishi Materials, with a nose radius of 0.4 mm, a nose angle of 60^o, a rake angle of 0^o and a thickness of 2.381 mm. Table 2 presents the limits of the input variables: rotation velocity (n) and feed rate (f).

The randomness of tests must be guaranteed in order to obtain results that are dependent only on input variables and non-influenced by tool wear. Considering an experimental design with 2 factors, 2 level each and 3 repetitions of each experiment, there are 4 experiments and 12 tests in total.

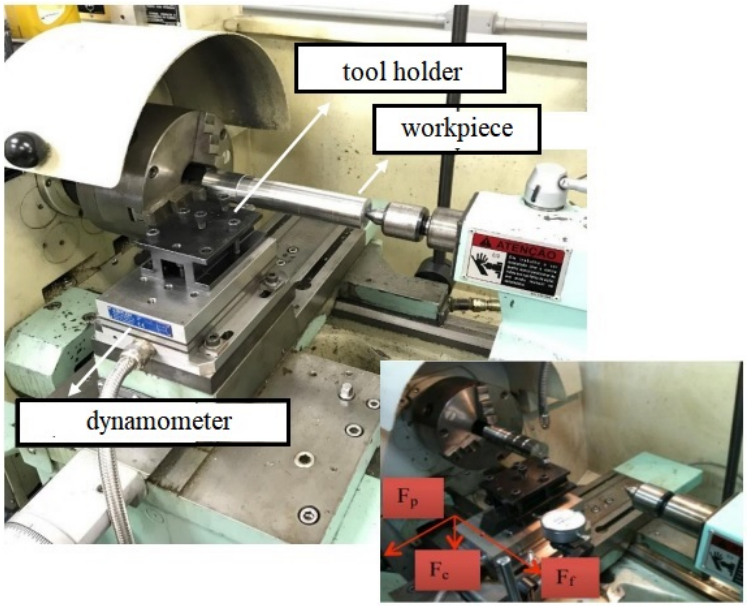

Figure 1 – Experimental set up.

Table 2 – Limit of input variables

	Parameter	Level 1	Level 2
P1	Rotation velocity (rpm)	500	800
P2	Feed rate (mm)	0.091	0.199

FRICTION CALCULATION

The acting forces during the machining process are divided into three pairs and each one is related to a shear zone. The first pair is formed by the tangential (F_r) and normal (F_N) force in the secondary shear zone (ZCS), the second pair is formed by the tangential (F_z) and normal (F_{nz}) force in the primary shear zone (ZCP) and the third is given in the tertiary shear zone (ZCT) formed by the force in the shear direction (F_c) and feed rate (F_f) on the cutting edge of the tool, as shown in Fig. 2.

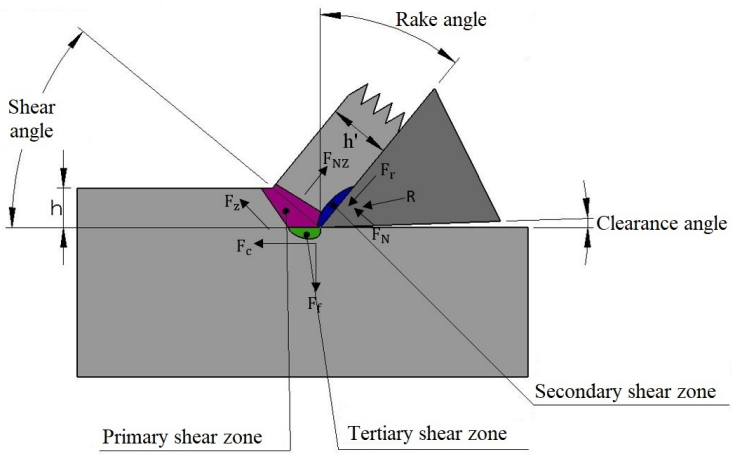

Figure 2 – Mechanism of chip formation with shear zones.

In the secondary shear zone, friction plays an important rule in the chip flow. Also, crater wear is formed, implying tool life decreasing. Using the Merchant model (Araujo *et al.*, 2020; Groover, 2012) for the orthogonal cutting model, the estimation of the friction angle β, the friction coefficient μ, the forces F_r and F_N and shear plane angle ϕ are presented in Eq. (4), (5), (6) and (7):

$$tg(\beta) = \mu = \frac{F_r}{F_N} \tag{4}$$

$$F_r = F_c sen(\gamma) + F_f cos(\gamma) \tag{5}$$

$$F_N = F_c cos(\gamma) - F_f sen(\gamma) \tag{6}$$

$$\phi = 45^o - \frac{\beta}{2} + \frac{\alpha}{2} \tag{7}$$

where α is the rake angle.

In Equations (5) and (6), forces F_c and F_f are the cutting and feed forces obtained by the dynamometer and γ is the tool rake angle. From Equation (8), it is possible to determine the friction coefficient with the feed rate (f) and cutting velocity (V_c) data.

$$ln\mu_{exp_i} = a_0 + a_1 lnf + a_2 lnV_c + a_3 ln(fV_c) \tag{8}$$

Solving the system in Eq. (9), it is possible to obtain the calibration coefficients of the mechanistic model (a_0, a_1, a_2, a_3) and, later, within the calibration limits, to obtain the friction evolution curve for each material.

$$\begin{bmatrix} 1 & -lnf_t^- & lnV_c^- & ln(f_t^- V_c^-) \\ 1 & -lnf_t^+ & lnV_c^- & ln(f_t^+ V_c^-) \\ 1 & -lnf_t^- & lnV_c^+ & ln(f_t^- V_c^+) \\ 1 & -lnf_t^+ & lnV_c^+ & ln(f_t^+ V_c^+) \end{bmatrix} \cdot \begin{bmatrix} a_o \\ a_1 \\ a_2 \\ a_3 \end{bmatrix} = \begin{bmatrix} \mu_{exp_1} \\ \mu_{exp_1} \\ \mu_{exp_1} \\ \mu_{exp_1} \end{bmatrix} \tag{9}$$

where the superscripts - and + are referring to the lower and upper levels of each planning parameters experimental, respectively. The mechanistic model of Eq. (8), calibrated from experimental data, is important to avoid the need for excessive experimental data when wants to know the machinability issues of a certain material within a select calibration limit.

After determining the parameters a_i, the friction coefficient for the superduplex steel is determined from AISI 316 and AISI 410 friction coefficients in the following equation. Separately, the material phases of AISI 316 and AISI 410 are representative of composition of the biphasic steel:

$$\mu_{sd} = a\mu_{316} + b\mu_{410} + c \tag{10}$$

NUMERICAL PROCEDURE

The numerical procedure is based on limit analysis theory considering friction at contact interface as stated in Figueiredo and Borges (2017, 2020). Limit analysis is a direct method based on plasticity theory. Limit analysis aims the determination of the plastic collapse power (in this case it is related to cutting forces), velocity and stresses fields, plastic strain rates and plastic dissipation. In the propose formulation, the occurrence of sticking/sliding regimes at tool-chip interface is determined from the distribution of contact stresses and tangential velocities. If sliding occurs, there is friction dissipation. Otherwise, there is sticking. If sticking occurs, material adheres to rake face and the secondary shear zone is formed.

In the computational model, the workpiece is treated as a deformable body, under the assumptions of elastic perfectly-plastic material, von Mises criteria and in a plane strain hypothesis. The tool is treated as a rigid body, not represent in the model. The contact interface is represented by unilateral conditions, assuming known and permanent contact and Coulomb friction law for tangential direction. The deformable body is discretized into triangular finite elements, considering quadratic interpolation for the velocity field and linear interpolation for the stress field.

In limit analysis, a permanent configuration is required. This configuration is determined from the Mechant's model Araujo *et al.* (2020); Groover (2012), considering the chip as continuous and straight. In orthogonal cutting, large deformation usually occurs. However, dissimilar to incremental analysis in which a load history is imposed and the geometry is updated at each load step, limit analysis deals with the phenomenon of imminent plastic collapse at a permanent regime configuration. In this case, this configuration is determined by Merchant model. In this context, limit analysis deals with strain rates (not strain) in an elastic perfectly-plastic material and the velocity field expresses a tendency of movement at plastic collapse. Limit analysis looks for this limit situation, after that large deformation may occur. The post plastic collapse response is not covered by this theory.

As shown in Figure 3, a velocity field is imposed in order to simulate the movement of the workpiece, while the cutting tool is stationary.

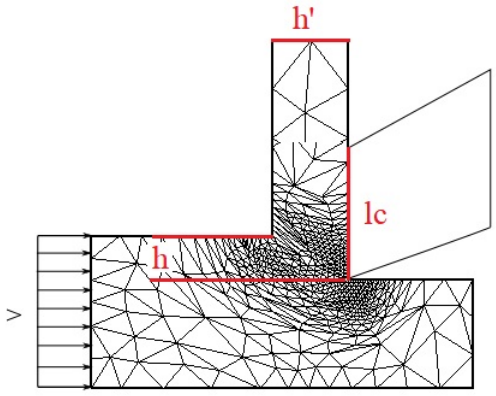

Figure 3 – Mesh generated for the numerical solution.

The contact lengths (l_c) are evaluated from Kachanov and Poletika's model (Grzesik, 2008), presented in the Eq. (11). Equation (11a) is dependent on the shear plane angle ϕ (Eq. (7)), whereas Eq. (11b) is dependent on the chip compression ratio is the ratio of the chip thickness (h') to the nominal thickness of the cut (h) (Grzesik, 2008):

$$l_c = \frac{2hcos\,(\gamma_o - \phi)}{sen\phi} \tag{11a}$$

$$\frac{l_c}{h} = 2\left(\frac{h'}{h}\right) \tag{11b}$$

where h' is measured from the Scanning Electron Microscope (SEM).

In order to generate the Merchant-based geometry, some parameters are necessary: cutting thickness (h = 0.091 mm e 0.199 mm); friction coefficient (μ); chip-tool contact length (l_c); rake angle surface (λ_0 = 0); rotation velocity (n = 800 rpm), chip thickness (h'), cut depth (a_p = 0.25 mm); cutting width determined by Waldorf (2006) model (w), as shown in Eq. (12), yield stress material (σ_y) and experimental cutting force for theses machining conditions ($F_{c_{exp}}$).

$$w = r_n\left(\frac{\pi}{2} - \chi' + sen^{-1}\left(\frac{f}{2r_n}\right)\right) + \frac{a_p - r_n\,[1 - sen(\chi')]}{cos(\chi')} \tag{12}$$

where χ' is the side cutting edge (lead) angle and r_n is the tool nose radius.

RESULTS AND DISCUSSIONS

In this section, the experimental machining forces for SS, AISI 316 and AISI 410 steels are presented. From these experimental forces, the friction coefficients are evaluated according to Merchant model. After that, the mechanistic model is applied and the calibration coefficients are determined.

The friction coefficients determined from these dissimilar methodologies are used in the numerical model.

Friction Calculation

Table 3 presents the averages of cutting (F_c), passive (F_p) and feed (F_f) forces for the three steels. From these experimental results, the friction coefficients were calculated by the Merchant's model for each machining condition, as indicated in Tab. 4. Finally, the calibration coefficients were calculate by the Eq. (9), as shown in Tab. 5.

Table 3 – Experimental results for machining forces

Exp.	f (mm)	n (rpm)	Superduplex Force (N)			AISI 316 Force (N)			AISI 410 Force (N)		
			F_c	F_p	F_f	F_c	F_p	F_f	F_c	F_p	F_f
A	0.091	500	67.84	48.08	28.99	63.97	44.69	23.93	57.10	32.50	22.59
B	0.199	500	107.26	72.04	31.75	109.93	76.76	29.11	94.23	69.17	28.70
C	0.091	800	68.14	50.56	30.71	68.04	48.71	26.94	55.25	31.39	23.62
D	0.199	800	101.63	72.90	30.39	92.55	65.29	22.09	77.77	50.00	23.12

Table 4 – Results of the friction coefficient calculation

Exp.	f (mm)	n (rpm)	μ_{SD}	μ_{316}	μ_{410}
A	0.091	500	0.4273	0.3741	0.3956
B	0.199	500	0.2960	0.2648	0.3046
C	0.091	800	0.4507	0.3959	0.4275
D	0.199	800	0.2990	0.2837	0.2973

Table 5 – Calibration coefficients for the homogeneous model

Aço	a_0	a_1	a_2	a_3
AISI316	-1.9358	-0.3460	0.1480	-0.1981
AISI410	-2.2189	-0.2850	0.1708	-0.1141
UNS S32760	-2.4495	-0.3537	0.2106	-0.1431

The results obtained from Tab. 5 does not provide a mechanistic relation between superduplex steel and AISI 410 ferritic and AISI 316 austenitic steels. In order to achieve this relation, the SS friction coefficient was determined from a linear function of AISI 316 and AISI 410, according to Eq. 10. The values of these new friction coefficients are present in Tab. 6.

Table 6 – Calibration coefficients for the linear model

a	b	c
0.4878	0.6870	0.0216

Figure 4 exhibits the friction coefficients curves for AISI 316, AISI 410 and superduplex stainless steels, considering a rotation velocity of 800 rpm. One can observe that the friction coefficient decreases with the increasing of chip thickness. This phenomenon can be explained by the mechanism of chip formation. It is known that the higher the tool feed rate is, considering a constant cut depth, the chip tends to be more discontinuous or broken. Thus, if the chip breaks easily, the contact area becomes smaller and so as the friction coefficient between formed chip and the rake surface of the tool.

In this figure, it should be emphasize the proximity of the curves by mechanistic and linear model for the superduplex steel. This proximity of the results indicates that it not necessary to machine UNS S32760 steel to obtain the friction

coefficient generated during the process. Experimental data from commercially low cost steels (compared to SS), such as AISI 316 and AISI 410, can be used, which simulate the ferrite and austenite phases contained in SS.

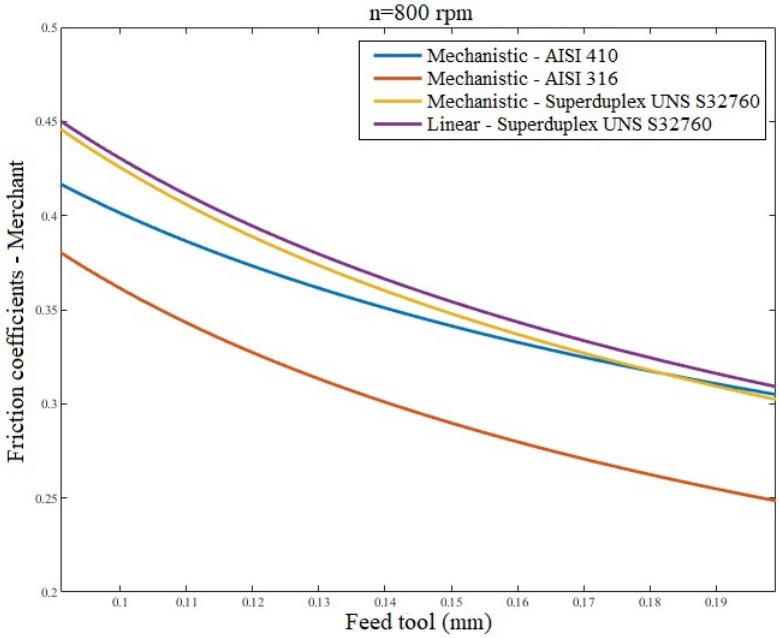

Figure 4 – Friction variation x feed rate.

The results for the experimental (obtained from Merchant's orthogonal cutting model), mechanistic and linear friction coefficients are presented in the Tab. 7, considering rotation of 800 rpm.

Table 7 – Friction coefficient results by the Merchant, mechanistic and linear model

Steel	h (mm)	μ_{exp}	$\mu_{mech.}$	μ_l
UNS S32760	0.091	0.4507	0.4460	0.4503
	0.199	0.2990	0.3023	0.3091

Numerical Procedure

Table 8 shows the experimental results for the cutting forces (F_c) obtained by the dynamometer during the cutting process. The cutting conditions and the contact lenghts are also presented. The deformed chip thickness h' was obtained using scanning electron microscope (SEM) as observed in Fig. 5.

The difference between the contact lengths determined from Kachanov models is due to friction angle ϕ and the deformed chip h'. In Eq. (11a), the friction angle ϕ is obtained from experimental forces while in Eq. (11b) the deformed chip is measured from SEM. In the last one, the chip curved shape may cause inaccurate results.

Table 8 – Results of chip-tool contact length calculation for Kachanov a and Kachanov b

Superduplex steel								
Data							l_c (mm)	
n	h (mm)	w (mm)	F_c	h' (mm)	K_h=h'/h	ϕ (rad)	Kach.a	Kach. b
800	0.0910	0.5691	68.14	0.1825	2.0054	0.5737	0.2817	0.3650
800	0.1990	0.5141	101.63	0.2067	1.0385	0.6401	0.5344	0.4134

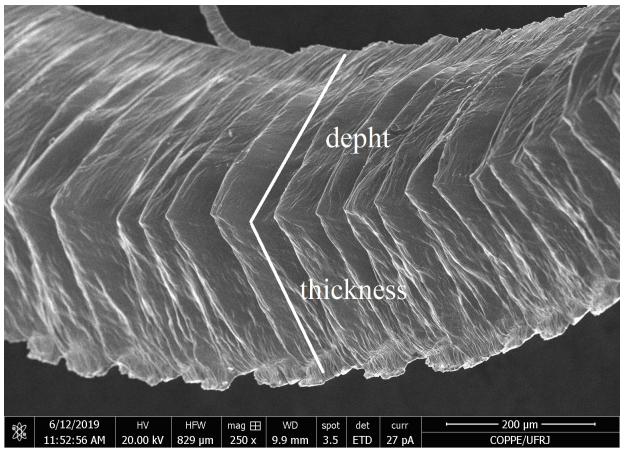

Figure 5 – SEM image of the chip formation

The data presented in Tab. 7 and Tab. 8 are used as inputs in the numerical model. The contact lengths were evaluated by Kachanov models (called Kach. a and Kach. b).

Table 9 – Cutting forces results by numerical model

Superduplex steel					
h (mm)	F_c (N)	l_c (mm)	μ	F_{num} (N)	Erro (%)
0.091	68	Kach. a	Experimental	46.49	31.77
			Mechanistic	46.36	31.96
			Linear	46.48	31.79
		Kach. b	Experimental	60.14	11.74
			Mechanistic	59.63	12.49
			Linear	60.08	11.83
0.199	102	Kach. a	Experimental	106.92	5.21
			Mechanistic	107.00	5.28
			Linear	105.42	3.73
		Kach. b	Experimental	99.28	2.31
			Mechanistic	99.46	2.14
			Linear	99.66	1.94

The results for cutting forces in Table 9 for the SS were obtained from AISI 316 and AISI 410 data. Besides cutting forces, the numerical model based on limit analysis theory provides the distribution of stress and velocity fields, the plastic multiplier (related to shear zones) and stresses and velocities at chip-tool contact:

Figure 6(a) presents the distribution of normal and tangential stresses at chip-tool contact. These results correspond to the case feed rate 0.199 mm, rotation velocity 800 rpm, experimental friction coefficient for Superduplex Steel. The origin of the local reference system is located at tool edge ($s/l_c = 0$). Both stresses are close to zero at s/l_c=1. It is coherent since in this point there is loss of contact between the chip and tool. Regarding the normal stresses, its maximum is reached near the tool edge and it decreases along the rake face, until the occurrence of chip-tool contact loss. In cutting process high normal stresses are developed. Figure 6(b) presents the distribution of tangential velocities at chip-tool contact. It is a relative velocity and one can observe that it is null at tool edge. On the rake face there is sliding occurrence and it implies friction dissipation at chip-tool contact interface. On the other hand, if null tangential velocities are observed at some part or entire rake face, there is material adhesion to tool rake face. If it occurs, the secondary shear zone is formed.

The velocity field and the primary and secondary shear zones are observed as follows:

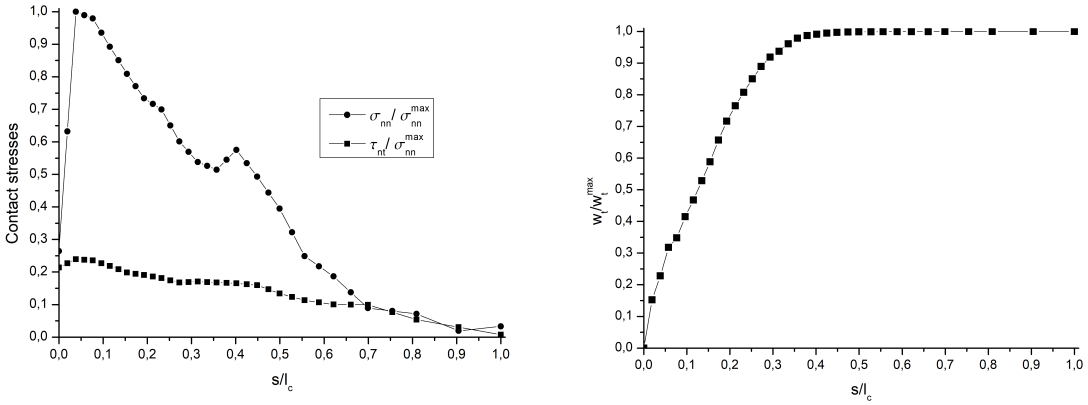

(a) (b)

Figure 6 – a) Normal (σ_{nn}) and tangential (τ_{nt}) stresses in the chip-tool contact and b) Tangential velocity by contact length evolution (s/l$_c$).

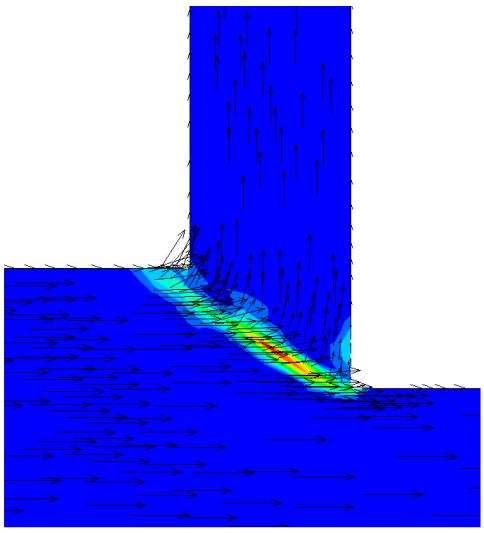

Figure 7 – Velocity field for n=800 rpm and f=0,199 mm.

Figure 7 shows the obtained velocity field for the proposed permanent regime configuration derived from the Merchant model. According to these results, there is a good agreement between the velocity vectors and the boundaries of the proposed geometry. One can also observe the primary shear zone. Due to a stagnation point at tool edge, a secondary shear zone is formed around this point. Since there is sliding at most points, there is friction dissipation at rake face.

CONCLUSIONS

The evaluation of experimental cutting forces is costly and time consuming, even costly if material presents low machining. Then, the use of numerical methods to simulate such process has been growing in interest in academia and industries. In machining, the prolonging of tool life is an important aspect in order to reduce production costs and friction at chip-tool interface plays an important rule in wear evaluation.

The main objective of this work is to evaluate the friction coefficient from experimental results. This estimation is based on Merchant and mechanistic models to predict the friction coefficient and the use of these results as an input for the numerical model based on limit analysis theory and finite element method. The use of a numerical model allows a

better understanding of the cutting process and analysis of local quantities, as distribution of contact stresses, occurrence of sliding/sticking and the determination of shear zones.

In spite of dealing with large deformation during the orthogonal cutting process, limit analysis theory looks for a imminent plastic collapse situation, in which large deformation may occur after this point. Dissimilar to incremental analysis, in which a configuration is updated ate each load step, limit analysis deals with a permanent regime configuration and strain rates (not strain) are calculated for a elastic perfectly-plastic material. In this sense, the obtained velocity field for the permanent geometry determined from Merchant model indicates a tendency of movement.

Regarding the numerical cutting forces calculated considering the cutting depths $h = 0.091mm$ and $h = 0.199mm$, regarding the methodologies Kachanov a and Kachanov b, the last ones present lower relative errors. For $h = 0.091mm$, the numerical cutting forces evaluated from experimental friction coefficient present the lowest relative error, 11.74% and close to the linear friction coefficient. Regarding $h = 0.199mm$, the linear model for friction coefficient provided the lowest relative error, 1.94%. Regardless of the feed rate, the linear model, which uses information from AISI 316 and AISI 410 steels to describe the phases present in the superduplex steel, was relevant because it obtained a satisfactory result in the value of the cutting forces.

The behavior of normal and tangential stresses in the chip-tool contact region was also observed. The normal contact stresses reaches a maximum near the cutting edge and decreases along the rake face, until reaching near zero when there is loss of chip-tool contact. This distribution is according to the contact length methodology proposed by Kachanov. The distribution of tangential velocities enables the analysis of sliding/sticking zones. For the obtained friction coefficients, there is sliding at most entire rake face, implying friction dissipation. Sticking occur around tool edge. However, as long as friction coefficient increases, due to lack of lubrication for example, sticking zones may advance across the rake face. If it occurs, chip does not flow over the rake face due to material adherence. In this case, adjacent material flows over the adhered portion entailing the secondary shear zone.

ACKNOWLEDGMENTS

The authors would like to acknowledge FAPERJ for the Technological Initiation grant that made possible the development of this research.

REFERENCES

Araujo, A.C., Mougo, A.L. and Campos, F.O., 2020, "Usinagem para engenharia: um curso de mecânica do corte", E-papers.

Fatima, A. and Mativenga, P.T., 2013, "A review of tool–chip contact length models in machining and future direction for improvement", Proceedings of the Institution of Mechanical Engineers, Part B: Journal of Engineering Manufacture, Vol. 227, No. 3, pp. 345–356.

Figueiredo, F.C. and Borges, L.A., 2017, "Limit analysis formulation for frictional problems", Archive of Applied Mechanics, Vol. 86, pp. 1965–1977.

Figueiredo, F.C. and Borges, L.A., 2020, "Limit analysis and frictional contact: formulation and numerical solution", Meccanica, Vol. 55, No. 6, pp. 1347–1363.

Groover, M.P., 2012, "Fundamentals of modern manufacturing: materials processes, and systems", John Wiley & Sons.

Grzesik, W., 2008, "Advanced machining processes of metallic materials: theory, modelling and applications", Elsevier.

Waldorf, D.J., 2006, "A simplified model for ploughing forces in turning", Journal of manufacturing processes, Vol. 8, No. 2, pp. 76–82.

RESPONSIBILITY NOTICE

The authors are the only parties responsible for the printed material included in this paper.